Microelectronics Reliability 50 (2010) 2012–2019

Contents lists available at ScienceDirect

Microelectronics Reliability

journal homepage: www.elsevier.com/locate/microrel

Application of RPN analysis to parameter optimization of passive components

K.S. Chen [a], C.C. Wang [b], C.H. Wang [b,*], C.F. Huang [a]

[a] Department of Industrial Engineering and Management, National Chin-Yi University of Technology, Taichung 411, Taiwan
[b] Institute of Manufacturing Information and Systems, National Cheng Kung University, No. 1, Ta Hsueh Road, Tainan 701, Taiwan

ARTICLE INFO

Article history:
Received 13 March 2010
Received in revised form 22 June 2010
Available online 31 July 2010

ABSTRACT

In the trend toward the development of electronic products that are compact and lightweight, as portable consumer electronic products, such as the cell phone, Bluetooth, GPS, W-LAN, digital camera, wireless phone, and notebook computer, increase in demand, the frequency control components needed for communications related industries receive increased attention. The crystal oscillator is widely used as a frequency selective passive component in communications related industries because of excellent characteristics, such as temperature stability and a low loss. A crystal oscillator consists mainly of a quartz crystal and an IC that controls the oscillation circuits, and is applied to high precision communications products, requiring high frequency accuracy. A crystal oscillator with an output frequency that deviates or is unstable will seriously degrade the quality and functionality of an expensive communications product.

This present research investigates the crystal oscillator manufacturing processes, developing risk priority number analysis specifically for critical-to-quality processes and identifying the optimum priority for improvements in the process quality. Using Taguchi experimental design techniques the optimal parameter design is determined for quality characteristics and a mathematic programming method establishes an objective mode for monitoring quality. Lastly, the present research uses a real case to verify the modes proposed in this project, to enhance customer satisfaction, and produce crystal oscillators with a competitive advantage.

1. Introduction

Since the invention of communication instruments, scientists and engineers have worked to develop new products that combine visuals, communications, and information. In this century of well developed communication technology, the trend of electronic product development is toward compactness and light weight. Portable consumer electronic products, such as the cell phone, Bluetooth, GPS, W-LAN, digital camera, wireless phone, and notebook computer are increasing in demand; as a result, the frequency control components are being paid more attention—the crystal oscillator (CXO), for instance, is widely used in communications related industries because it has excellent characteristics, such as temperature stability and a low loss.

Quartz crystals are electronic passive components made of quartz that offer frequency stability during high frequency oscillation. Presently, quartz crystals are widely used in all kinds of electronic products and systems, including those in military, communications, and consumer electronic categories. According to International Data Corporation (IDC), a market survey institution, in 2009, communications applications accounted for 45% of CXO usage, information technology accounted for 30%, and consumer electronics and others accounted for the remaining 25%. Communications applications predominate mainly because the continuous and rapid worldwide growth of cell phone sales worldwide with the advent of very affordable phones. The increasing precision and diversity of cell phone functions demand that the quartz components also increase in quantity and quality. For example, a CXO is the frequency control component in the Apple iPod and iPhone, HTC Touch Diamond, Mediatek's chips for cell phones, the Intel Centrino module, ASUS motherboards, and Seagate hard disk drives. The market for related applications of CXO products is divided into a great number of categories (as shown in Fig. 1), and will be even more diversified in future.

The CXO consists primarily of a quartz crystal and an IC that controls the oscillation circuits, as shown in Fig. 2. A CXO can be classified according to its frequency control method and accuracy as: a common crystal oscillator (CXO); voltage controlled crystal oscillator (VCXO); temperature compensated crystal oscillator (TCXO); and digitally compensated crystal oscillator (DCXO). The classification and application areas are shown in Table 1. According to Buck [1] and Deno et al. [2], as CXOs are applied in communication products of higher precision, they require very high precision frequencies. At normal room temperature, the frequency precision can be as low as ±100 ppm; but if the output frequency of quartz

* Corresponding author.
E-mail address: thomas_6701@yahoo.com.tw (C.H. Wang).

0026-2714/$ - see front matter © 2010 Elsevier Ltd. All rights reserved.
doi:10.1016/j.microrel.2010.06.014

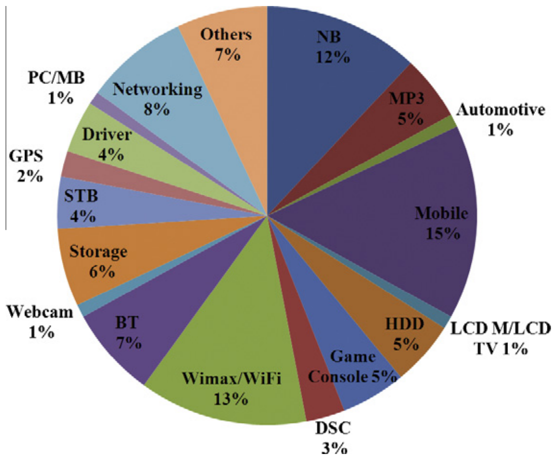

Fig. 1. Diagram of the market distribution of products containing a CXO.

crystal deviates or is unstable, its influence on the quality and functions of the expensive communication product would be severe. Consequently, each step of the manufacturing processes of a CXO is crucial.

The chief CXO components are the quartz crystal, controller IC, and ceramic package. The CXO manufacturing processes can be divided into front end, where the frequency is adjusted, and back end processes, which provide function testing. The front end processes begins with cutting, grinding, and cleaning a quartz crystal bar used as a piezoelectric material into blanks, followed by coating gold (Au) or silver (Ag) materials on the blank surface by evaporation deposition. Wire bonding welds gold wires on the IC and the ceramic package; an auto mounting process attaches the driving blanks to the ceramic package surface, followed by frequency adjustment to the target frequency; a seam spot process then welds a nickel lid on the ceramic package to prevent exterior environmental pollution and damage. The back end processes of function testing apply aging, leak testing, and electrical characterization through final quality control, marking, packing, and shipping. Fig. 3 roughly shows the CXO manufacturing processes.

Because passive components, such as crystal oscillators, are applied in high precision and high priced communication products they must operate at the desired frequency with a very high degree of precision. For example, the maximum drift in the central target frequency has changed from the range of ±100 ppm at −40–85 °C to presently within ±15 ppm, which provides great room for improvement, as well as many difficulties. Hence, every CXO manufacturing process is crucial and the process quality and yield rates deserve careful investigation—any deviation or instability in the CXO output frequency would seriously affect the quality and functionality of the end products. A poor quality CXO could lead to a massive loss of purchase orders.

Therefore, it is a matter of utmost importance that any enterprise wishing to strengthen its competitive edge internationally, take the satisfaction of customers seriously by engaging the quality characteristics of CXO products. If firms continuously search out

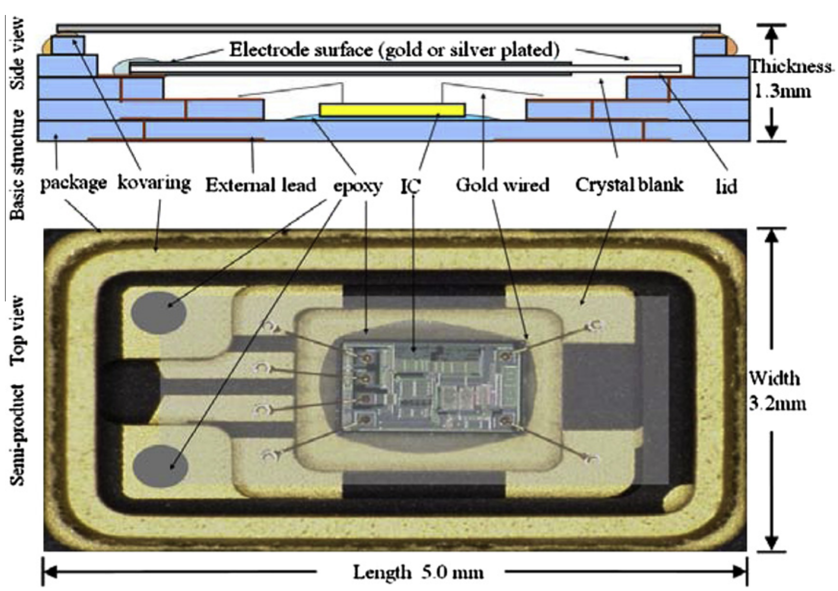

Fig. 2. Basic structure of CXO packaging.

Table 1
CXO classification and application areas.

Type of CXO	Precision (coefficient of frequency/temperature)	Typical applications
Common crystal oscillator (CXO)	10^{-4}–10^{-5}	Computer, camcorder, hard disk drive
Voltage controlled crystal oscillator (VCXO)	10^{-4}–10^{-5}	Phase lock loop
Temperature compensated crystal oscillator (TCXO)	10^{-6}	Cell phone, GPS
Digitally compensated crystal oscillator (DCXO)	10^{-8} (with 10^{-10} per g option)	Standard frequency for navigation system clock rate, MTI radar, satellite terminal radar

Remarks: precision (coefficient of frequency over temperature).

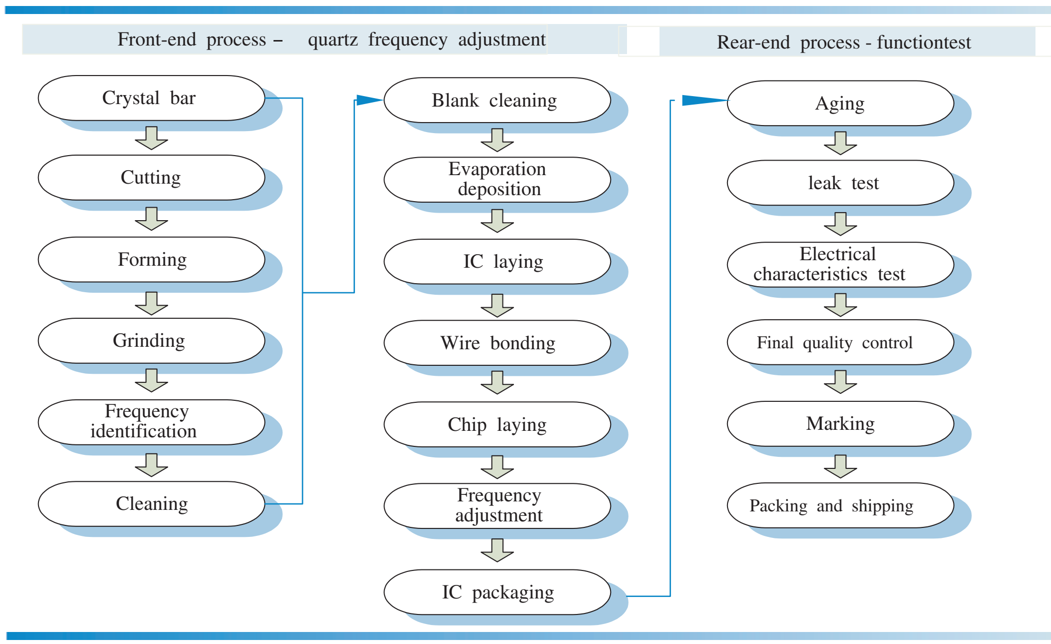

Fig. 3. Diagram of CXO manufacturing processes.

ways to improve manufacturing processes and optimize process parameters, the quality characteristics of CXO products will increase. Based on these fundamentals, the present research analyzes the processes of CXO, and risk priority number, RPN, for critical-to-quality processes. To determine the priority of key processes for the improvement in the quality of CXO, the present research employs Taguchi method to identify the optimal design parameters for processes with key quality characteristics, before utilizing mathematical planning, to validate the results of such identification. In this manner, it is possible to enhance customer satisfaction, and the international competitiveness of related industries.

2. Analysis of CXO failures

As stated above, CXO should undergo three tests before being packed and shipped: temperature testing, leak testing, and electrical characterization testing. Of these tests, the electrical characterization test is the most important. If CXO failed this test, the product would be usable, but unable to function as designed. Failure to pass the electrical characterization test may be closely associated with prior-to-packaging processes such as evaporation deposition, IC laying, wire bonding, chip laying and frequency adjustment. Therefore, every process must achieve a high level of quality before CXO's utility can be assured. This study uses risk priority number (RPN) to analyze the order of improvements in the enhancement of CXO quality of the process.

According to Chao and Ishii [3], RPN rates the problems quantitatively, between 1 and 10, according to the aspects of occurrence, detection and severity. In evaluation, RPN = occurrence × detection × severity, with the resulting value falling anywhere between 0 and 1000. The higher the risk is, the higher the value will be; representing higher priority in the order of required improvements. To that end, the present research evaluated the five above-stated processes according to the underlying conditions of the three CXO test procedures. This study determined the RPN, defining their risk index as $R_i = O_i \times D_i \times S_i$, $i = 1, 2, 3, 4, 5$, where O_i = occurrence, D_i = detection, and S_i = severity. The present research identified the priority of processes for improvement based, on the results of RPN analysis, detailed as follows.

2.1. Occurrence

During the process of CXO, the product underwent evaporation deposition, IC laying, wire bonding, chip laying and frequency adjustment, and the quality of each affected the function and test results of the product. The quality characteristics of evaporation deposition, IC laying and frequency adjustment were identified as nominal-the-best; deviation of wire bonding was smaller-the-better type. According to Davis [4] and Chen et al. [5], the process capabilities of all quality characteristics should meet the requirements before basic customer requirements can be satisfied. Overall, when the capability of a process is stronger, the process yield rate is higher and, by the concept of Taguchi function of loss, process loss is lower, and failure is less likely. Accordingly, the present research used a bilateral specification index, S_{pk}, and an unilateral specification index, C_{pu}, to reflect the probability of failure.

Many process capability indices, such as C_p, C_{pk}, C_{pm} and C_{pmk}, measure the nominal-the-best type quality characteristics. None of these indices has a one-to-one relationship with process yield% and therefore, none can accurately reflect the value of the process. Consequently, Boyles [6] proposed a bilateral specification index, S_{pk}, that can provide a one-to-one relationship with process yield% and more accurately measure the process performance. This index is defined as follows:

$$S_{pk} = \frac{1}{3}\Phi^{-1}\left\{\frac{1}{2}\Phi\left(\frac{\text{USL}-\mu}{\sigma}\right) + \frac{1}{2}\Phi\left(\frac{\mu-\text{LSL}}{\sigma}\right)\right\} \quad (1)$$

where $\Phi(x)$ is standard normal cumulative distribution function, and USL and LSL are upper and lower limits, respectively. When $S_{pk} = c$, the relationship between S_{pk} and process yield rate, yield% = 2Φ (3c)-1. Apparently, index S_{pk} had a one-to-one relationship with the process yield rate. With S_{pk}, Huang et al. [7] developed an assessment model for analyzing the process capability of a backlight module. In addition, Kane [8] proposed an index, C_{pu}, that could measure smaller-the-better type quality characteristics, and had a one-to-one relationship with process yield rates under the assumption of normal state conditions, that is, yield% = $\Phi(3C_{pu})$. This index was defined by the following:

$$C_{pu} = \frac{\mathrm{USL} - \mu}{3\sigma} \tag{2}$$

It appeared that when the capability of a process were stronger, the loss of the process was lower and failure was less likely. Accordingly, the present research used bilateral specification index, S_{pk}, and unilateral specification index, C_{pu}, to reflect the probability of occurrence of failure. Through the relationships, $k\sigma = d$ and $(\mu - T)/d \leqslant 1.5/k$, proposed by Pearn and Chen [9] and Chen et al. [10], calculated the S_{pk} and C_{pu} values corresponding to quality levels, represented by k Sigmas, and the corresponding level (O_i) of occurrence rate of failure (Table 2). It appears that a smaller O_i meant a higher quality level (k), greater S_{pk} and C_{pu} values, and lower likelihood of failure.

2.2. Detection

The purpose of detection, D_i, was to determine whether it were possible to detect the cause of a failure. We could determine the cause of a defective CXO, based on the combination of temperature test (T_1), leak test (T_2) and electrical characterization test (T_3). We can let t_j be the test value for T_j, i.e., $T_j = t_j$, where $t_j = 0$ represents passing the test, and $t_j = 1$ failing to pass the test, $j = 1, 2, 3$. In fact, a failure to pass the electrical characterization test (T_3) would indicate a defective CXO, and passing the electrical characterization test (T_3) would indicate a passable product, even if both the temperature test (T_1) and leak test (T_2) indicated failure. As such, t the CXO must fail the electrical characterization test to fail the CXO testing procedure. Therefore, reviewing the causes of a defective CXO must be conducted only after the electrical characterization test ($T_3 = 1$) has failed. The probability of detection could thus be defined as $P(I = i|T_1 = t_1, T_2 = t_2, T_3 = 1) = d_i(t_1, t_2)$, where $d_i(t_1, t_2)$ was the actual evaluation of probability of detection, i being process 1, 2, . . . , 5. The quality and reliability established by engineers, was based on the opinions and experience of the on-site manufacturing operators, as well as data collected from sample inspections by QC personnel. These were determined through statistic calculation and analysis via the table of detection probability (Table 3).

From Table 3, we could easily find the probability of detection for any process. For example, with a failed electrical characterization test, we could test and determine the probability of a defective CXO resulting from the evaporation deposition process in the below cases.

Case 1: to determine the probability of defective CXO due to the evaporation deposition process at 0.43 (i.e., $d_1(0, 0) = 0.43$), with both temperature test and leak test having been passed (i.e., $t_1 = 0$, $t_2 = 0$).
Case 2: to determine the probability of defective CXO due to the evaporation deposition process at 0.52 (i.e., $d_1(0, 1) = 0.52$), with the temperature test having been passed ($t_1 = 0$) but the leak test failed ($t_2 = 1$).
Case 3: to determine the probability of defective CXO due to the evaporation deposition process at 0.60 (i.e., $d_1(1, 0) = 0.60$), with the temperature test having been failed ($t_1 = 1$) but the leak test passed ($t_2 = 0$).
Case 4: to determine the probability of defective CXO due to the evaporation deposition process at 0.79 (i.e., $d_1(1, 1) = 0.79$), with both the temperature test and leak test having been failed (i.e., $t_1 = 1$, $t_2 = 1$).

Through comparison with Table 3, we can divide the detection probabilities into 10 levels, as in:

$$D_i = f\{d_i(t_1, t_2) = y\} = b, \quad y \in \left(\frac{b}{10}, \frac{b+1}{10}\right), \quad b = 1, 2, 3 \ldots 10 \tag{3}$$

For example, in Case 1 above (i.e., $t_1 = 0$, $t_2 = 0$), the probability of defective CXO due to the evaporation deposition process was found to be 0.43, that is, $y = 0.43$; since the value of y was somewhere between $b/10$ and $(b + 1)/10$, it derived $b = 4$, meaning detection $D_i = 4$.

2.3. Severity

S_i stands for severity; it stresses the importance of the effect leading to a failure, that is, it represents how each process affects

Table 2
Evaluation of occurrences.

Quality level	Index value		O_i
$6.0 \leqslant k$	$1.55 \leqslant S_{pk}$	$1.50 \leqslant C_{pu}$	1
$5.5 \leqslant k < 6.0$	$1.39 \leqslant S_{pk} < 1.55$	$1.33 \leqslant C_{pu} < 1.50$	2
$5.0 \leqslant k < 5.5$	$1.23 \leqslant S_{pk} < 1.39$	$1.17 \leqslant C_{pu} < 1.33$	3
$4.5 \leqslant k < 5.0$	$1.07 \leqslant S_{pk} < 1.23$	$1.00 \leqslant C_{pu} < 1.17$	4
$4.0 \leqslant k < 4.5$	$0.91 \leqslant S_{pk} < 1.07$	$0.83 \leqslant C_{pu} < 1.00$	5
$3.5 \leqslant k < 4.0$	$0.76 \leqslant S_{pk} < 0.91$	$0.67 \leqslant C_{pu} < 0.83$	6
$3.0 \leqslant k < 3.5$	$0.61 \leqslant S_{pk} < 0.76$	$0.50 \leqslant C_{pu} < 0.67$	7
$2.5 \leqslant k < 3.0$	$0.47 \leqslant S_{pk} < 0.61$	$0.33 \leqslant C_{pu} < 0.50$	8
$2.0 \leqslant k < 2.5$	$0.34 \leqslant S_{pk} < 0.47$	$0.17 \leqslant C_{pu} < 0.33$	9
$k < 2.0$	$S_{pk} < 0.34$	$C_{pu} < 0.17$	10

Table 3
Detection probabilities of various processes.

	(T_1, T_2) Process			
	(0, 0)	(0, 1)	(1, 0)	(1, 1)
1. Evaporation deposition	$d_1(0, 0) = 0.43$	$d_1(0, 1) = 0.52$	$d_1(1, 0) = 0.60$	$d_1(1, 1) = 0.79$
2. IC laying	$d_2(0, 0) = 0.18$	$d_2(0, 1) = 0.21$	$d_2(1, 0) = 0.38$	$d_2(1, 1) = 0.46$
3. Wire bonding	$d_3(0, 0) = 0.41$	$d_3(0, 1) = 0.71$	$d_3(1, 0) = 0.77$	$d_3(1, 1) = 0.92$
4. Chip laying	$d_4(0, 0) = 0.15$	$d_4(0, 1) = 0.23$	$d_4(1, 0) = 0.27$	$d_4(1, 1) = 0.46$
5. Frequency adjustment	$d_5(0, 0) = 0.21$	$d_5(0, 1) = 0.48$	$d_5(1, 0) = 0.32$	$d_5(1, 1) = 0.36$

Table 4
Classification of the severity of processes.

Process	Description	Severity
1. Evaporation deposition	Potential of seriously affecting the product	8
2. IC laying	Has medium level of effects on the product or downstream process	5
3. Wire bonding	The effect of failure is serious and causes non-conformity	9
4. Chip laying	Significantly affects the process and may need rework or repair	6
5. Frequency adjustment	Has minor effect on product or downstream processes, probably without being noticed	3

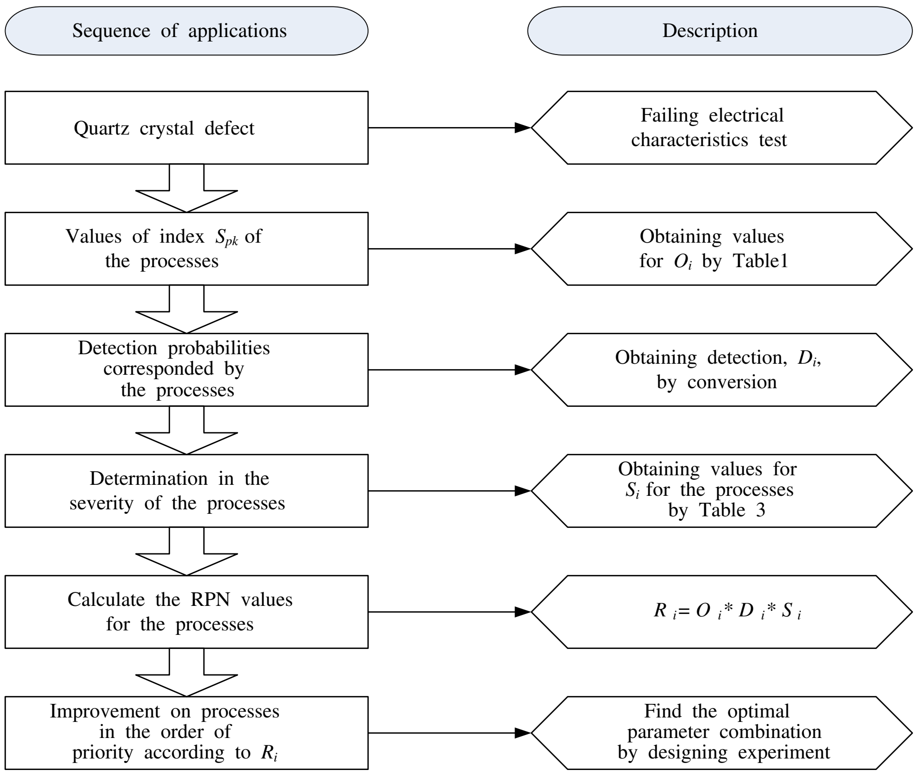

Fig. 4. Flow diagram of the RPN application.

the degree of failure. Out of the 10 severity levels, level 1 represents the failure of a process that does not significantly affect the final product (a severity with no effect); level 2 represents that the process affects the product very slightly. Similarly, level 10 represents hazardous severity—the failure condition caused by the process is serious. By this definition for severity classification, the five processes are given ratings, as Table 4 shows, in this research after discussions with the manufacturing units and the product testing units.

From the above RPN definitions and descriptions, a higher value for R_i meant that the process would need a higher priority for improvement, where $1 \leqslant R_i = O_i \times D_i \times S_i \leqslant 1000$. The present research has now reorganized the RPN applications as shown in Fig. 4. From sampling data collected from the firm, it was found that after three test processes, the CXO failed the electrical characterization test resulting in a defective CXO; although the CXO passed the temperature test, it did not pass the leak test; thus, the detection probability was $d_i(0, 1)$. From Tables 2–4, and Eq. (3), we obtain the CXO failure analysis results shown in Table 5; the RPN result determined that the wire bonding process required priority for improvement.

3. Taguchi experimental design

As stated above, the R_i value of 441 for the process wire bonding was apparently higher than the R_i values for any of the other four processes; hence, this process rated the first priority in improvement. Following that, a case was needed for analysis and improvement specifically on the wire bonding process, given that numerous parameters affect the size of the wire sweep. It was pointed out by Pande et al. [11] and Goh et al. [12] that, in general, the tools commonly used in analysis are the cause-and-effect diagram, Gantt chart, process capability analysis, and quality function deployment. Chen et al. [10] and Huang et al. [13] used cause-and-effect diagrams to analyze the causes of poor performance of TFT-LCD and surveillance cameras processes and improved them with satisfactory results. Hence, the cause-and-effect diagram was used in this research as a tool for analyzing the size of the wire sweep, as shown in Fig. 5.

Table 5
Analysis results for CXO processes.

Process	Index (O_i)	$d_i(0, 1)$ (D_i)	S_i	R_i	Priority
1. Evaporation deposition	5	0.52 (5)	8	200	2
2. IC laying	4	0.21 (2)	5	40	5
3. Wire bonding	7	0.71 (7)	9	441	1
4. Chip laying	3	0.23 (2)	6	36	4
5. Frequency adjustment	4	0.48 (4)	3	48	3

Based on the above cause-and-effect diagram and summarizing discussions with the people in charge of project improvement and the process team, the present research discovered that molding temperature in equipment, wire length among geometric properties, time to fill molds and the viscosity of plastic filler were the major factors affecting the size of the wire sweep. According to Ross [14] and Taguchi [15], Taguchi experimental design determines design parameters in an experimental manner, by selecting the appropriate orthogonal arrays to use, based on the number of controlling factors and their levels. It then reduced interactions, by replacing quality loss functions with S/N, and was capable of providing product design and quality with robustness with the least amount of time, the lowest cost and the fewest repetitions of the experiment. To obtain improved design parameters, the present research utilized Taguchi method to analyze design of experiments.

As stated above, the present research selected the controlling factors and their levels, as shown in Table 6, with regard to the analytic results of the size of the wire sweep, and identified the optimal parameter design by Taguchi design of experiments. In this experiment, there were four 3-level factors, with eight degrees of freedom. Therefore, we adopted the $L_9(3^4)$ orthogonal array, which was one of the orthogonal arrays Dr. Taguchi recommended

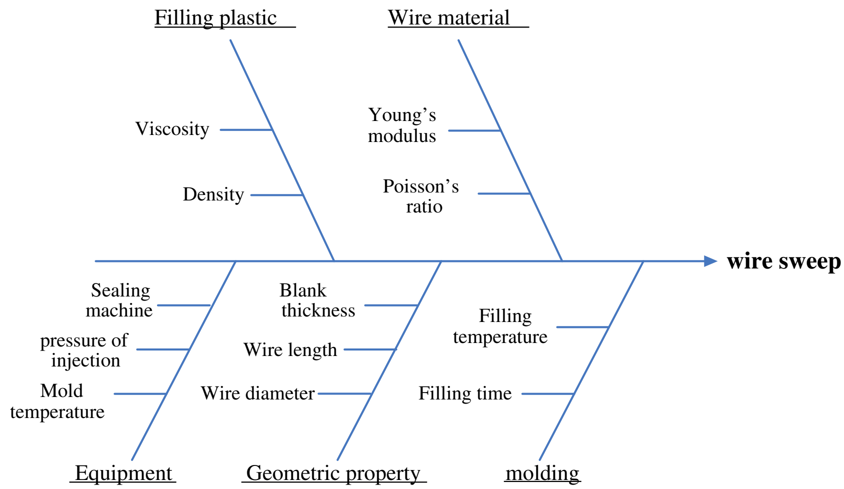

Fig. 5. Cause-and-effect diagram of the size of the wire sweep.

Table 6
Table of controlling factor levels.

	Factor	Level 1	Level 2	Level3
A	Viscosity, poise	175	200	225
B	Wire length (mm)	2.25	2.5	2.75
C	Filling time (s)	12	17	22
D	Mold temperature (°C)	140	155	160

Table 7
Experimental results in $L_9(3^4)$ orthogonal arrays.

Experiment number	Parameters and levels				Result	
	A	B	C	D	mm	*S*/*N*
1	1	1	1	1	0.442	7.092
2	1	2	2	2	0.352	9.069
3	1	3	3	3	0.311	10.145
4	2	1	2	3	0.322	9.843
5	2	2	3	1	0.312	10.117
6	2	3	1	2	0.621	4.138
7	3	1	3	2	0.194	14.244
8	3	2	1	3	0.682	3.324
9	3	3	2	1	0.553	5.145

highly (Taguchi [16]). Our $L_9(3^4)$ orthogonal array is shown in Table 7, which also gives the results of the experiment.

As Taguchi [16] pointed out, *S*/*N* refers to signal to noise ratio. A higher *S*/*N* ratio indicates a higher signal value compared to that of noise. Consequently, it is easier to tell which has been received: signal or noise. *S*/*N* ratio was obtained by logarithmic conversion of loss function, as the criteria for measuring product performance, mainly for reducing interactions to enhance product robustness. It is expressed as follows:

Table 8
Table of reaction of design factors to the *S*/*N* ratio.

	A	B	C	D
Level 1	8.768	10.393	4.851	7.451
Level 2	8.033	7.503	8.019	9.150
Level 3	7.571	6.476	11.502	7.771
Effect	1.197	3.917	6.651	1.699
Rank	4	2	1	3

$$SN = -10\log\left[\frac{1}{n}\sum_{i=1}^{n}\frac{1}{y_i^2}\right] \tag{4}$$

By using Eq. (4), we could obtain the *S*/*N* ratio of each from the experiment results listed in Table 7. The higher such *S*/*N* ratio was, the smaller size of the wire sweep was representing higher quality level in the wire process. Now by using the *S*/*N* ratios listed in Table 7, we could obtain the average *S*/*N* values for the four factors at every level, as shown in Table 8.

A higher value for factors in Table 8 meant a higher reaction in that design factor to the *S*/*N* ratio. Lastly, this data is plotted in Fig. 6, and we obtain the design combination of factors A1, B1,

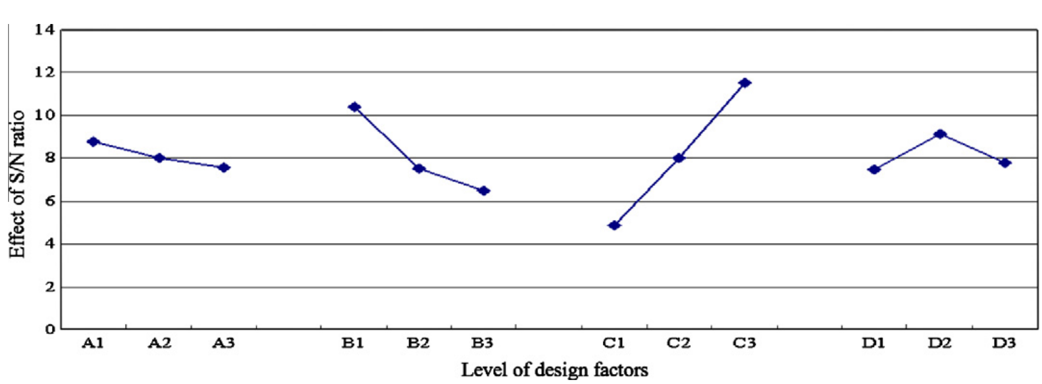

Fig. 6. Table of the relation of design factors to the *S*/*N* ratio.

C3, and D2 as the optimal parameter design, to minimize the size of the wire sweep.

4. Verifying and monitoring the experimental results

The control factors affecting the size of the wire sweep included viscosity, wire length, filling time, and mold temperature. In this research, the Taguchi experimental design found that the combination of factors A1, B1, C3, and D2 generated the smallest size of the wire sweep. Next, we will verify the experimental results, conducting confirmation experiments using the optimal design of combination A1B1C3D2 and an original design of A2B2C2D2, under the same conditions to compare the process capabilities of the two. Cheng [17] and Pearn and Chen [18] pointed out that it is necessary to obtain estimations at the indices, since process parameters are unknown, and that as samples are not error free, they cannot objectively determine whether the level requirement is met by the index estimation alone. Hence, the use of joint confidence intervals to replace index estimation in indicating the process capability of wire bonding is more objective. Because the size of the wire sweep is a the smaller-the-better quality characteristic, while index C_{pu} evaluates a unilateral process and index C_{pu} is a function of δ and γ, where δ and γ can be regarded as the process parameters of relative specifications, the definition of C_{pu} is re-expressed as:

$$C_{pu}(\delta,\gamma)=\frac{\text{USL}-\mu}{3\sigma}=\frac{1-\delta}{3\gamma},\quad \text{where } \delta=\mu/\text{USL} \text{ and } \gamma=\sigma/\text{USL} \tag{5}$$

Since the distribution of probability of index C_{pu} is very complex, yet the $100(1-\alpha)\%$ joint confidence intervals for δ and γ can be obtained easily, they can be induced by Boole's inequality as:

$$\delta=(\delta_L,\delta_U)=\left\{\hat{\delta}-\frac{\hat{\gamma}}{\sqrt{n}}t_{n-1,\alpha/4},\hat{\delta}+\frac{\hat{\gamma}}{\sqrt{n}}t_{n-1,\alpha/4}\right\}, \tag{6}$$

$$\gamma=(\gamma_L,\gamma_U)=\left\{\sqrt{\frac{(n-1)\hat{\gamma}^2}{\chi^2_{n-1,\alpha/4}}},\quad\sqrt{\frac{(n-1)\hat{\gamma}^2}{\chi^2_{n-1,1-\alpha/4}}}\right\} \tag{7}$$

Obviously, the chance of the actual process (δ,γ) falling within the $100(1-\alpha)\%$ joint confidence interval of δ and γ, $S=(\delta_L,\delta_U)\times(\gamma_L,\gamma_U)$ is very good. Hence, this research uses index $C_{pu}(\delta,\gamma)$ as the target index and the $100(1-\alpha)\%$ joint confidence interval of δ and γ, S as a constraint, i.e., a feasible region, and applies a mathematical programming method to find the maximum and minimum of $C_{pu}(\delta,\gamma)$, which are the confidence intervals of index $C_{pu}(\delta,\gamma)$; the graph (Fig. 7) and general form are expressed as:

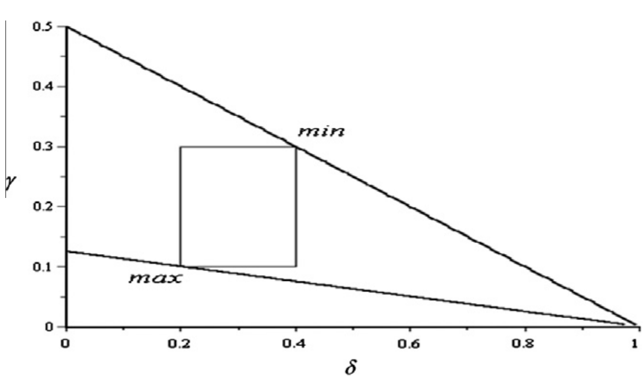

Fig. 7. Diagram of the relationship between the objective and the constraints.

$$\begin{cases}\max C_{pu}(\delta,\gamma) & (1)\\ s.t.\ \delta_L\leqslant\delta\leqslant\delta_U & (2)\\ \gamma_L\leqslant\gamma\leqslant\gamma_U & (3)\end{cases} \tag{8}$$

$$\begin{cases}\min C_{pu}(\delta,\gamma) & (1)\\ s.t.\ \delta_L\leqslant\delta\leqslant\delta_U & (2)\\ \gamma_L\leqslant\gamma\leqslant\gamma_U & (3)\end{cases} \tag{9}$$

Since the probability of δ and γ falling in the set, S, obtained by mathematical programming is $(1-\alpha)$, the solution of the maximum and minimum in $S=(\delta_L,\delta_U)\times(\gamma_L,\gamma_U)$ is as good as determining the upper and lower limits of confidence for the index $C_{pu}(\delta,\gamma)$. Thus, we solve the 95% confidence intervals for the index C_{pu} in the original design and the optimal design, respectively; the calculation from Eqs. (8) and (9) is:

A2B2C2D2:

$$\begin{cases}\max(\min)\ C_{pu}(\delta,\gamma)=\frac{1-\delta}{3\gamma}\\ s.t.\ 0.1796\leqslant\delta\leqslant 0.2876\\ 0.3389\leqslant\gamma\leqslant 0.4752\end{cases}$$

A1B1C3D2:

$$\begin{cases}\max(\min)\ C_{pu}(\delta,\gamma)=\frac{1-\delta}{3\gamma}\\ s.t.\ 0.1273\leqslant\delta\leqslant 0.2627\\ 0.2156\leqslant\gamma\leqslant 0.3024\end{cases}$$

According to these results, the joint confidence intervals of δ and γ for combination 1 (A2B2C2D2) are $\delta=(0.1796, 0.2867)$ and $\gamma=(0.3389, 0.4752)$; and those for combination 2 (A1B1C3D2) are $\delta=(0.1273, 0.2627)$ and $\gamma=(0.2156, 0.3024)$. Next, the mathematic programming method was applied to solve for index C_{pu} for its 95% confidence intervals C_{pu}. Consequently, the 95% confidence interval for C_{pu} in combination 1 (A2B2C2D2): $S_1=[0.5004, 0.8070]$, and that in combination 2 (A2B2C2D2): $S_2=[0.8127, 1.3490]$.

Solving the confidence interval of index C_{pu}, using Eqs. (6) and (7) could result in joint confidence intervals for δ and γ, and it make it easier to obtain two sets of confidence intervals for index C_{pu}, $S_1=[L_1, U_1]$ and $S_2=[L_2, U_2]$; by the intersection of these two sets, we could tell how strong the two process capabilities were. From the 95% confidence intervals for the process capability index C_{pu} in combination 1 (A2B2C2D2): $S_1=[0.5004, 0.8070]$, and combination 2 (A2B2C2D2): $S_2=[0.8127, 1.3490]$, which were obtained from the sampling data of the above stated the original design and optimal design, it was determined that $S_1\cap S_2$ was an empty set. If the intersection of the two confidence intervals were an empty set, this would represent a significant difference between the two process capabilities. Since $U_1=0.8070<L_2=0.8127$ (Fig. 8), the optimal combination obtained through Taguchi experiment design had significantly improved the process capability of wire bonding.

Without a loss of generality, the present research solved the $C_{pu}(\delta,\gamma)$ confidence intervals by mathematical programming in the following steps:

Step 1: determine significant levels (generally $\alpha=0.05$ or 0.01).
Step 2: calculate sample average ($\bar{X}$) and standard deviation (S) of the original design and optimal design combinations, respectively.
Step 3: calculate δ and γ values for the original design and the optimal design.
Step 4: calculate δ and γ joint confidence intervals (δ_L,δ_U) and (δ_L,δ_U) for the original design and the optimal design.
Step 5: solve 95% confidence interval combinations S_1 and S_2 for the $C_{pu}(\delta,\gamma)$ by mathematical programming.

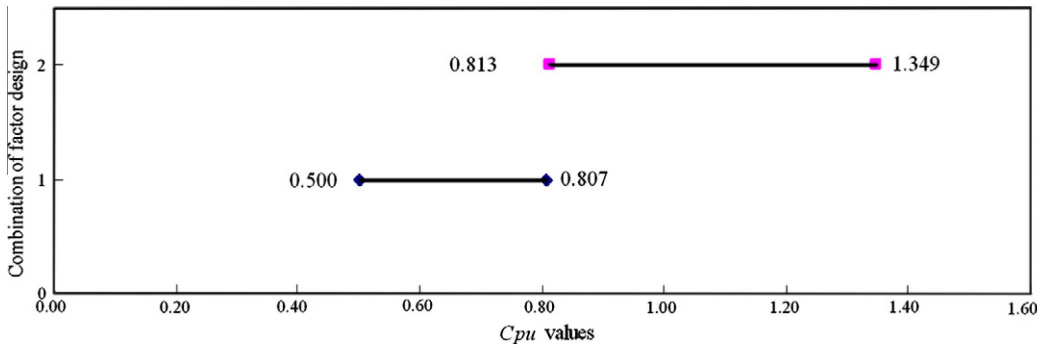

Fig. 8. Comparison of confidence intervals for the indices C_{pu} of the two processes.

Step 6: by the intersection of combinations $S_1 = [L_1, U_1]$ and $S_2 = [L_2, U_2]$, determine whether the process capabilities exceed:

(1) $S_1 \cap S_2 = \psi$, then the process capabilities significantly differ in two different ways:
  a. $U_1 < L_2$, then process capability $S_1 < S_2$.
  b. $U_2 < L_1$, then process capability $S_1 > S_2$.

(2) $S_1 \cap S_2 \neq \psi$, then the process capabilities do not differ notably.

5. Conclusions

This research successfully combined process capability indices that are widely used in many industries and the risk priority number (RPN), and utilized the concept of RPN to propose a complete evaluation model for application to the quartz crystal industry. First, the occurrence, detection, and severity for each CXO manufacturing process was evaluated, where the occurrence was divided by the process yield rate, S_{pk}, and unilateral specification index, C_{pu}; detection was defined as $P(I = i|T_1 = t_1, T_2 = t_2, T_3 = 1) = d_i(t_1, t_2)$ according to the relationship among the temperature test (T_1), leak test (T_2), and electrical characteristics test (T_3). After evaluating the occurrence, detection, and severity of each process, the RPN values for each process were obtained. In this research, these RPNs facilitated the determination that the wire bonding process needed priority in improvement. We determined the factors affecting the size of the wire sweep with a cause-and-effect diagram and obtained the optimal parameter combination by the Taguchi design of experiments; the experimental results were verified with confidence intervals for index C_{pu}. Finally, by examining index C_{pu}, we determined the critical values for monitoring the process quality and enabling the customer to assess whether the wire bonding process complied with the requirements. Through this complete evaluation method, this research not only can clearly determine the process capabilities, detection probability, and the severity of effect of a failure on the final product, but also conducts a synthesized assessment of CXO processes using RPN. As such, it is possible to analyze the causes of failure specifically of the processes with high RPNs; this assists the industry in effectively engaging itself in process improvement, and obtaining optimal improvements in a timely manner.

References

[1] Buck DL. Digital design for a self-temperature compensating oscillator. IEEE Int Freq Control PDA Exhibit 2002:615–43.
[2] Deno S, Hehnlen C, Landis D. A low cost microcontroller compensated crystal oscillator. IEEE Freq Control Sympos 1997:954–60.
[3] Chao LP, Ishii K. Design process error proofing: failure modes and effects analysis of the design process. J Mech Des 2007;129(5):491–502.
[4] Davis RB. A capability study for an entire product. ASQC Qual Congr Trans 1992:172–8.
[5] Chen KS, Pearn WL, Lin PC. Capability measures for processes with multiple characteristics. Qual Reliab Eng Int 2003;19:101–10.
[6] Boyles RA. Process capability with asymmetric tolerances. Commun Stat: Comput Simul 1994;23:615–43.
[7] Huang ML, Chen KS, Hung YH. Integrated process capability analysis with an application in backlight. Microelectron Reliab 2002;42:2009–14.
[8] Kane VE. Process capability indices. J Qual Technol 1986;18:41–52.
[9] Pearn WL, Chen KS. Multi-process performance analysis: a case study. Qual Eng 1997;10(1):1–8.
[10] Chen KS, Wang CH, Chen HT. A MAIC approach to TFT-LCD panel quality improvement. Microelectron Reliab 2006;46:1189–98.
[11] Pande PS, Neuman RP, Gavanagh RR. The six sigma way. McGraw-Hill; 2000.
[12] Goh TN, Low PC, Tsui KL, Xie M. Impact of six sigma implementation on stock price performance. Total Qual Manage Bus Excell 2003;14(7):753–63.
[13] Huang CT, Chen KS, Chang TC. An application of DMADV methodology for increasing the yield rate of surveillance cameras. Microelectron Reliab 2010;50:266–72.
[14] Ross PJ. Taguchi techniques for quality engineering. New York: McGraw-Hill; 1988.
[15] Taguchi G. Introduction to quality engineering. White Plains, New York: Asian Productivity Organization, UNIPUB; 1991.
[16] Taguchi G. System of experimental design: engineering methods to optimize quality and minimize cost. White Plains, New York: UNIPUB; 1987.
[17] Cheng SW. Practical implementation of testing process capability indices. Qual Eng 1994–1995;7:239–59.
[18] Pearn WL, Chen KS. One-sided capability indices C_{pu} and C_{pl}: decision making with sample information. Int J Qual Reliab Manage 2002;19(3):221–45.